THE ASTROPHYSICAL JOURNAL, 479:859–867, 1997 April 20

A SEARCH FOR TeV COUNTERPARTS TO BATSE GAMMA-RAY BURSTS

V. CONNAUGHTON,[1,2] C. W. AKERLOF,[3] S. BARTHELMY,[4] S. BILLER,[5] P. BOYLE,[6] J. BUCKLEY,[1] D. A. CARTER-LEWIS,[7] M. CATANESE,[7] M. F. CAWLEY,[8] T. CLINE,[4] D. J. FEGAN,[6] J. FINLEY,[9] G. J. FISHMAN,[2] J. GAIDOS,[9] N. GEHRELS,[4] A. M. HILLAS,[5] C. KOUVELIOTOU,[2] F. KRENNRICH,[7] R. C. LAMB,[7] R. LESSARD,[6] J. MCENERY,[6] C. MEEGAN,[2] G. MOHANTY,[7] N. A. PORTER,[6] J. QUINN,[6] A. RODGERS,[5] H. J. ROSE,[5] F. SAMUELSON,[7] M. S. SCHUBNELL,[3] G. SEMBROSKI,[9] R. SRINIVASAN,[9] T. C. WEEKES,[1] C. WILSON,[9] AND J. ZWEERINK[7]

Received 1996 August 7; accepted 1996 November 6

ABSTRACT

Intense effort has gone into the observation of optical, radio, and X-ray gamma-ray burst (GRB) counterparts, either simultaneous to the burst or as quasi-steady lingering remnants. Here we report on a similar study at higher energies of 250 GeV and above using ground-based telescopes. The recent technical advances represented by the atmospheric Cherenkov imaging technique (Cawley & Weekes 1995) have opened up the field of gamma-ray astronomy above 250 GeV and raised the possibility that these techniques can be used with excellent fluence sensitivity in exploring the GRB phenomenon. Observations by the Whipple collaboration of nine BATSE positions, one acquired within 2 minutes of the reported BATSE burst time, using coordinates distributed through the BATSE Coordinates Distribution Network (BACODINE) are reported. No evidence of TeV emission is found, and upper limits to the high-energy delayed or extended emission of observed candidates are calculated.

Subject headings: gamma rays: bursts — methods: data analysis

1. INTRODUCTION

Imaging atmospheric Cherenkov telescopes have achieved great sensitivity (Cawley & Weekes 1995) and now complement observations by orbiting telescopes such as those on the *Compton Gamma Ray Observatory* (*CGRO*). Previous studies of bursts by the Whipple collaboration (Connaughton et al. 1994), combined with recent improvements to the telescope, indicate that sensitivity above 250 GeV to a fluence of 6×10^{-9} ergs cm^{-2} can be achieved. The scientific benefits of the detection of a TeV component to a classical gamma-ray burst (GRB) would be the following: (1) it would constrain the particle acceleration models for the sources and provide valuable insights into the source radiation mechanisms; (2) it would set an upper limit to the source distance because of the predicted absorption of TeV photons by pair production with intergalactic infrared photons (Stecker et al. 1992) (i.e., eliminate deep cosmological models); (3) it would give a more accurate measure of the location of the burst and thus contribute to source identification; and (4) it would open a new window to the study of GRB phenomena from the ground.

The discovery of a delayed component in some bursts (Hurley et al. 1994a) by the Energetic Gamma-Ray Experiment Telescope (EGRET) instrument on *CGRO* implies that a long observation window may be available at high energies for at least some of the bursts observed by the Burst and Transient Source Experiment (BATSE) detectors, so that response time does not need to be instantaneous. A simple extrapolation from the observed delayed flux in the 1994 February 17 burst suggests that more than 10^4 photons should be seen in a half-hour observation by the Whipple 10 m reflector. Bright bursts, therefore, would be easily seen providing the spectra extended to TeV energies; fainter ones would also be detectable depending on their time structure and the accuracy to which they were located. It is difficult to compile spectra for the five individual bursts seen in the EGRET tracking detector (Hurley 1996) because the low number of photons involved introduces a large uncertainty, but the hardest, a spectral index of -2.0 obtained for the 1993 January 31 burst (Dingus et al. 1994), is encouraging. An average spectral analysis over the five combined bursts suggests that the spectrum above 30 MeV is flatter than suggested by BATSE measurements below 30 MeV. The fluence appears to be at least 15% of the BATSE fluence, but it could be much larger and remain undetected because of the 100 ms dead time of EGRET.

The persistence of high-energy emission over the duration of BATSE bursts, and perhaps beyond their decline, forces models for bursters to incorporate mechanisms that either continuously accelerate particles to these energies or produce particles whose lifetime is longer than the BATSE burst duration. If the GeV emission comes from the same source region as the sub-MeV photons, beaming factors must be high to account for the escape of GeV photons from the high-density radiation areas required to produce such bursts.

2. COUNTERPARTS AND THE BATSE COORDINATES DISTRIBUTION NETWORK (BACODINE)

Archival searches or follow-up observations to GRB at other wavelengths to look for emission concurrent with, or

[1] Center for Astrophysics–Whipple Observatory, P.O. Box 97, Amado, AZ 85645.
[2] Current address: NASA/Marshall Space Flight Center, ES 84, AL 35812.
[3] University of Michigan, Department of Physics, Randall Laboratory, Ann Arbor, MI 48109.
[4] NASA/Goddard Space Flight Center, Code 661, Greenbelt, MD 20706.
[5] University of Leeds, Department of Physics, Leeds LS2 9JT, England, UK.
[6] University College Dublin, Physics Department, Belfield, Dublin 4, Ireland.
[7] Iowa State University, Department of Physics and Astronomy, Osborn Drive, Ames, IA 50011.
[8] St. Patrick's College, Department of Experimental Physics, Maynooth, Kildare, Ireland.
[9] Purdue University, Department of Physics, Lafayette, IN 47907.

as a remnant of, the mechanism that produced the GRB may provide the breakthrough in the GRB puzzle. Implications and probabilities of finding counterparts and spectral features for burst distance scales are given by Hurley (1996). A comprehensive review of expected low-energy counterparts—flaring, fading, and quiescent—for most burst model types and an account of searches until 1993 for such radiation are given by Schaefer (1994).

Since its inception in 1993, the BATSE Coordinates Distribution Network (BACODINE) has provided a new way to look for activity from locations consistent with BATSE bursts (Barthelmy et al. 1994). The process of accumulating, transmitting, and processing the data from BATSE takes between 3.45 and 5.5 s, with an additional delay for transmission to follow-up observers. BACODINE provides the astrophysical community with the opportunity to make directed observations of burst positions. Some experiments, such as the wide-angle optical telescopes at Livermore (GROCSE) (Akerlof et al. 1994, 1995) have made almost simultaneous observations but have not been able to probe beyond the 8th magnitude. Other overlaps have been achieved serendipitously, particularly by instruments with wide sky coverage, such as air-shower detectors operating above 100 TeV. A reported positive detection by Plunkett et al. (1995) occurs well after the end of the burst, and its statistical significance is questionable in view of the low and irregular event rate shown over a 200 minute period. Edwards et al. (1995) report an overlap between their detector and the EGRET-detected 1993 January 31 burst, in which they found no PeV excess. This resulted in an upper limit to PeV emission from this burst that was lower than that obtained by extending the EGRET $E^{-2.0}$ spectrum to PeV energies. Since PeV burst activity concurrent with the BATSE trigger or as late as 1000 s afterward would have been apparent in that analysis, the result implies either a spectral cutoff or softening, or an extragalactic ($z > 0.05$) origin.

Hurley (1996) stresses the importance of a TeV counterpart in view of the detection of delayed or extended GeV emission by EGRET following BATSE bursts. Any TeV component would suffer attenuation through pair production with extragalactic background photons (Stecker et al. 1992), and a detection would exclude large cosmological distances as an origin for that burst. EGRET detections at about 1 GeV energies imply a source distance of less than $z \sim 80$ (Dingus et al. 1994) because of extinction of GeV photons by pair production on the cosmic microwave background. Although the cross section for this interaction increases with burst photon energy, the pair production of burst photons on the more local higher energy intergalactic background photons becomes dominant above a few GeV. There exist large uncertainties in the form of intergalactic photon fields, but the detection of an 18 GeV photon by EGRET confines the origin of this burst to within $z \sim 5$ regardless of the field model used. For TeV photons the extinction by pair production occurs at lower distances, mainly from interactions with infrared photons. Using Stecker's model for the infrared background, for example, the gamma-ray horizon for a 1 TeV photon lies at a redshift of $z = 0.09$ for a field that is assumed not to evolve with time or $z = 0.08$ assuming primordial evolution of the intergalactic field. A 200 GeV photon has its horizon at $z = 0.62$ (no evolution) or 0.41 (primordial evolution of the field). These values assume an $\Omega = 1$ cosmology with a Hubble constant of 50 km s^{-1} Mpc^{-1}. For a higher Hubble constant the limiting redshift is slightly higher.

Studies of the temporal profiles of the weakest relative to the strongest BATSE bursts have been used to infer time dilation factors $(1 + z_{\rm dim})/(1 + z_{\rm bright})$ of about 2 (Norris et al. 1994, 1995). If the bright bursts are nearby ($z_{\rm bright} \sim 0$), then this is consistent with the dimmest bursts we see with BATSE lying at $z_{\rm dim} \sim 1$–2. Cohen & Piran (1995) calculate that the most likely maximum redshift seen by BATSE is 2.1. If, however, the bright bursts are also distant and their spectra redshifted, then the dimmest bursts may lie at $z_{\rm dim} > 6$ (Fenimore & Bloom 1995). The maximum redshift value also varies according to intrinsic luminosity variations between bursts and source number evolution (Horack, Emslie, & Hartmann 1995).

If we are restricted by the optical depth of the intergalactic field to TeV photons to seeing only the nearest bursts, then even if the brightest GRB originate at $z \sim 0$, Whipple should detect at most one counterpart per year (Mannheim, Hartmann, & Funk 1996). If more are seen, or if a TeV counterpart to a weak (hence distant) BATSE burst is found, then a possible single-population cosmological origin for GRB would be eliminated. If a counterpart is not found, however, no conclusions can be drawn about distance scales or mechanisms, since the TeV component may (1) be too faint to be detected, (2) occur before any TeV instrument begins looking at the burst position, (3) exist at the source but disappear through attenuation, or (4) not exist. A null serendipitous observation concurrent with a well-defined interplanetary network (IPN) location (Hurley et al. 1994b) of a strong burst detected by BATSE and EGRET in the GeV range would eliminate option (2) and constrain galactic burst production model spectra (options 1 and 4), but a positive detection meaning that TeV emission exists and that we can see it would have enormous implications for distance scales and burst production mechanisms.

3. SEARCHES FOR TeV COUNTERPARTS TO BATSE BURSTS

3.1. *Search Technique*

The wide variety of burst types observed by BATSE and other detectors in terms of duration, temporal structure, and spectral features makes it difficult to characterize the appearance of a GRB signal at TeV energies. Since the origin of GRB is unknown, directed observations at a point in the sky in the hope of finding a burster are inappropriate, and the small field of view of the 10 m reflector (3°) makes a sky survey for bursts impractical. Follow-up observations to BACODINE notifications use information that is nearly simultaneous to the BATSE burst in order to monitor locations that have just seen burster activity. The Whipple collaboration joined BACODINE in the middle of 1994 and receives its notifications on an electronic mail account. This means there can be some delay between the detection of the burst by BATSE and the response by the Whipple collaboration.

The Cherenkov telescope has maximum sensitivity at the zenith but can be used down to elevations of 20° (Kifune et al. 1993; Krennrich et al. 1997) (as the elevation decreases, the energy threshold increases, as does the collection area); hence, roughly one-third of the sky is visible. The duty cycle of the Cherenkov telescope is limited by Sun, Moon, cloud, and instrument downtime to around 7%. Based on the fre-

quency of BATSE bursts (0.8 day^{-1}), our duty cycle, and sky coverage (above 20° elevation), we expect to receive one observable burst notification every 1.5 months.

Some recent technical developments at the Whipple Observatory increase the feasibility of a burst detection. A filter has been developed that permits the operation of the telescope under moonlight, thus effectively doubling the duty cycle (Chantell et al. 1995). To reduce the response time between notice of a burst and the commencement of observations, the azimuth drive of the telescope has been upgraded to increase the slew speed by a factor of 5. With this improvement we are now able to slew the telescope about 1° s^{-1}, so that data can be acquired within 5 minutes of burst notification.

The small field of view of the 10 m reflector means that the positional error box given by BATSE may not be completely covered at once, and this was a major consideration when developing a strategy for dealing with BACODINE information. The current method is to slew to the BATSE coordinates upon notification, so that the BACODINE position lies in the center of the field of view. This location is observed for one 28 minute scan, after which four positions 3° away from the first are monitored for 28 minutes each. A final 28 minute period is spent on the initial position, and the process is repeated the next evening for control purposes. It is not essential to make the control observations the next night; it is important only that the same positions be monitored through the same range of telescope elevations under similar sky conditions. Figure 1 shows the sky coverage achieved over the 3 hr observing cycle, along with the average BATSE error box.

3.2. *BACODINE Observations*

The burst account has received 50 BACODINE notifications since the Whipple collaboration joined the network in 1994 May. Of these, 16 arrived during the summer break/upgrade periods of 1994 and 1995, 25 arrived during bad weather or while the Moon was up, and nine were acted on by the Whipple observers. In five instances a full cycle of observations on the night of the burst and a full set of control data on another night were obtained. On other nights on which observations were made, the BACODINE position was setting, or dawn or moon rise were close to the notification time. The details of each burst monitored are given in Table 1.

BACODINE locations and intensities (I) are calculated from detector counts accumulated over the first 2 s of the event. On average, the size of the box (Δ) that will contain approximately 95% $\pm$ 5% of all BACODINE locations relative to the Huntsville locations at any given intensity I in counts per second above threshold energy (20–50 keV) integrated over the first 2 s is given by

$$\Delta = \sqrt{(8854 \times I^{-0.8577})^2 + 1.6^2}. \quad (1)$$

This equation is purely empirical, based on the set of overlapping detections between BACODINE and the complete Huntsville record. The power-law term represents a counting statistics contribution, and the fixed 1°.6 term represents an approximate underlying systematic contribution. All BATSE locations are limited by this systematic error, so that final Hunstville locations also contain this uncertainty, but since the final determined positions can incorporate photon directions from the entire burst, they are considered more accurate. The Huntsville locations are now provided routinely several days after the burst. An IPN location may also be calculated if the burst was bright enough to be seen in instruments on different platforms from BATSE. Bursts 3649, 3658, 3909, 3918, and 4048 in Table 1 were seen on more than one platform, and the most probable locations derived from the intersection of error boxes from the various instruments were 4°.7, 0°.22, 9°.49, 5°.72, and 2°.65 away from the BACODINE positions, respectively. The burst on 1995 June 25 occurred at the Galactic center during good weather. Sky conditions were not clear enough to make the control observations on the following few nights, and the burst position was not observable after that.

3.3. *Analysis of BACODINE Data*

Since the position of the BATSE burst given in the BACODINE notice has a statistical error that is pro-

TABLE 1

WHIPPLE OBSERVATIONS OF BACODINE POSITIONS

	BACODINE		HUNTSVILLE			WHIPPLE		
DATE	Trigger Number[a]	Intensity (counts s^{-1})[b]	Distance (deg)[c]	Error (deg)[d]	Duration (s)[e]	Delay (minutes)[f]	Elevation (deg)[g]	Cycles (1–6)[h]
1994 May 16.....	2980	630	11.8	6.2	4	19	24–14	1 (1 hr)
1995 Apr 05	3494	704	9.4	9.9	0.12	8	27–33	1, 2, 3
1995 May 24.....	3598	8726	1.4	2.2	6	5	56–31	Complete
1995 Jun 25.....	3649	1661	3.8	1.7	40	18	28–41	1–6
1995 Jul 01.....	3658	9134	2.3	1.6	15	56	41–69	Complete
1995 Nov 17.....	3909	1955	10.1	2.5	25	5	30–24	1 (1 hr)
1995 Nov 19.....	3911	801	6.7	7.1	60	20	45–54	Complete
1995 Nov 24.....	3918	1231	5.9	2.0	150	2	59–76	Complete
1995 Dec 20	4048	6698	2.8	1.7	17	27	71–37	Complete

[a] Trigger number of BATSE burst.

[b] Number of counts s^{-1} measured by BATSE in the first 1 or 2 s of the burst.

[c] Angular difference between the burst coordinates provided through BACODINE and the final estimated burst position from Huntsville.

[d] Error on final Huntsville location (statistical and systematic, 68% confidence limit).

[e] Duration of the burst seen by BATSE.

[f] Time elapsed between BACODINE message and start of first Whipple run.

[g] Average elevations of first and last positions covered by the 10 m telescope.

[h] Whipple coverage of burst area. The six positions are shown in Fig. 1. An entry of "complete" means that all 6 positions (plus control runs) were completed.

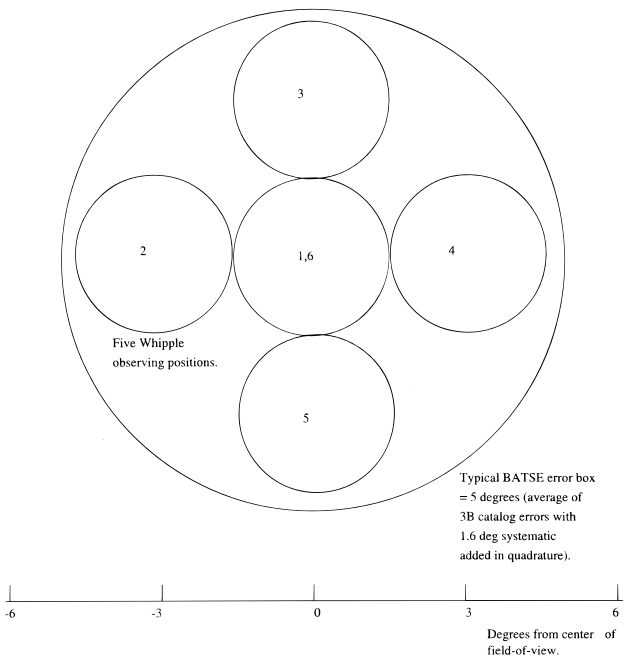

FIG. 1.—Response to BACODINE notification. Each circle represents the field of view of the 10 m reflector at different positions following a BATSE burst. The numbers in the circles indicate the sequence of observations. The centers of the circles are 3° apart, and the center of the first observation is at the coordinates given for the BATSE burst. There is some overlap between the observations, since the instrument is sensitive to showers from sources outside the geometrical field of view. A typical BATSE location error box is also shown.

portional to the intensity and a systematic error of 1°.6, the burster may lie anywhere in the five areas of monitored sky, or it could fall outside of the field of view. Because of the unknown potential duration of each burst at TeV energies, the whole image-selected data set is considered a potential burst. In effect, for each potential burst position monitored, a steady source over 28 minutes is being sought. The analysis must allow a search for a point source emitting at an unknown time over an unknown duration in one of the six data files. It must, therefore, first assume that each location on the sky contains a potential burster and look for an excess of gamma-ray–like events in each of the 28 minute scans from some point in the field of view, over the entire 28 minutes. The six data files taken on the night of each burst are the "ON" source data, and the control files are the "OFF" source data. The excess at any point in the ON data is found relative to the corresponding point in the control observations.

Events in the data files are comprised of the digitized signals registered by the 109 photomultiplier tubes in the focus box of the 10 m reflector. A moment analysis technique is used to fit an ellipse to each event, and the ellipse is characterized by a set of shape and orientation parameters. In this analysis, gamma-ray–like events are selected on the basis of image shape, using *width* (semiminor axis of ellipse) and *length* (semimajor axis) cuts. The development of image selection criteria and assessment of non–source-centered capabilities of the 10 m reflector are given in Connaughton et al. (1996). For geometric reasons, most BACODINE bursts occur close to the horizon, and the 3 hr observing cycle means that a wide range of telescope elevations is generally observed. Because of this, the ranges of *widths* and *lengths* that determine shape-selection cuts are defined by the average elevation of each data run. Above 35°, standard Supercuts shape criteria (Reynolds et al. 1993) are applied; below this, shape cuts optimized on 30° simulations are used. A minimum *size* (equal to the total light in digital counts of fitted image) of 400 is required for each event, corresponding to an energy threshold of around 0.3 TeV.

After isolating gamma-ray–like images, the most likely point of origin for each event is found using $d = 1.7$–1.7 (*width*/*length*) as the distance d away from the center of light along the major axis of the image (Akerlof et al. 1991). Light cones have been in place since the 1993–1994 season, and the operating threshold is lower, resulting in slightly different image characteristics; thus the distance of 1°.7 used in preference to the 2° specified in Connaughton et al. (1996) arises because of the different camera configurations involved (Lessard et al. 1996). This algorithm yields two points, one on either side of the center, and no effort is made to choose one of these on the basis of image asymmetry. Although the position of the burst is unknown, the most likely points of origin for incident gamma rays are defined to within the angular resolution of the technique. In this analysis the burst timescale is 28 minutes, and seeking a common point of origin for all shape-selected events would lead to much combinatorial noise (Akerlof et al. 1991). Instead, a grid of bins 0°.1 × 0°.1 in size is constructed to cover the field of view of the camera and beyond. The grid extends 5° on each side of the center, so that the sensitivity of the technique outside the geometrical field of view can be exploited. Each bin that lies within 0°.3 of either point of origin for an event is incremented in accordance with the efficiency of the common point-of-origin calculation described in Connaughton et al. (1996). This is repeated for the control data, and by comparing the occupancy levels of

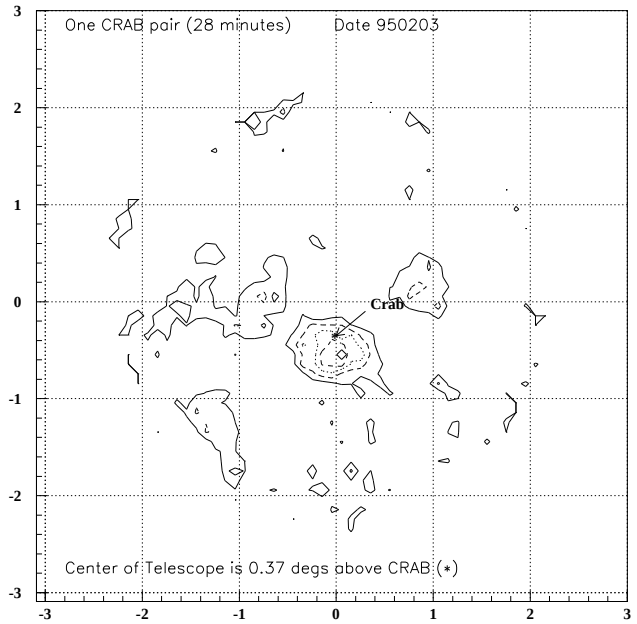

FIG. 2.—Distribution of bin excesses for one Crab Nebula pair after applying Supercuts *width* and *length* cuts. The arrow points to the position of the Crab Nebula.

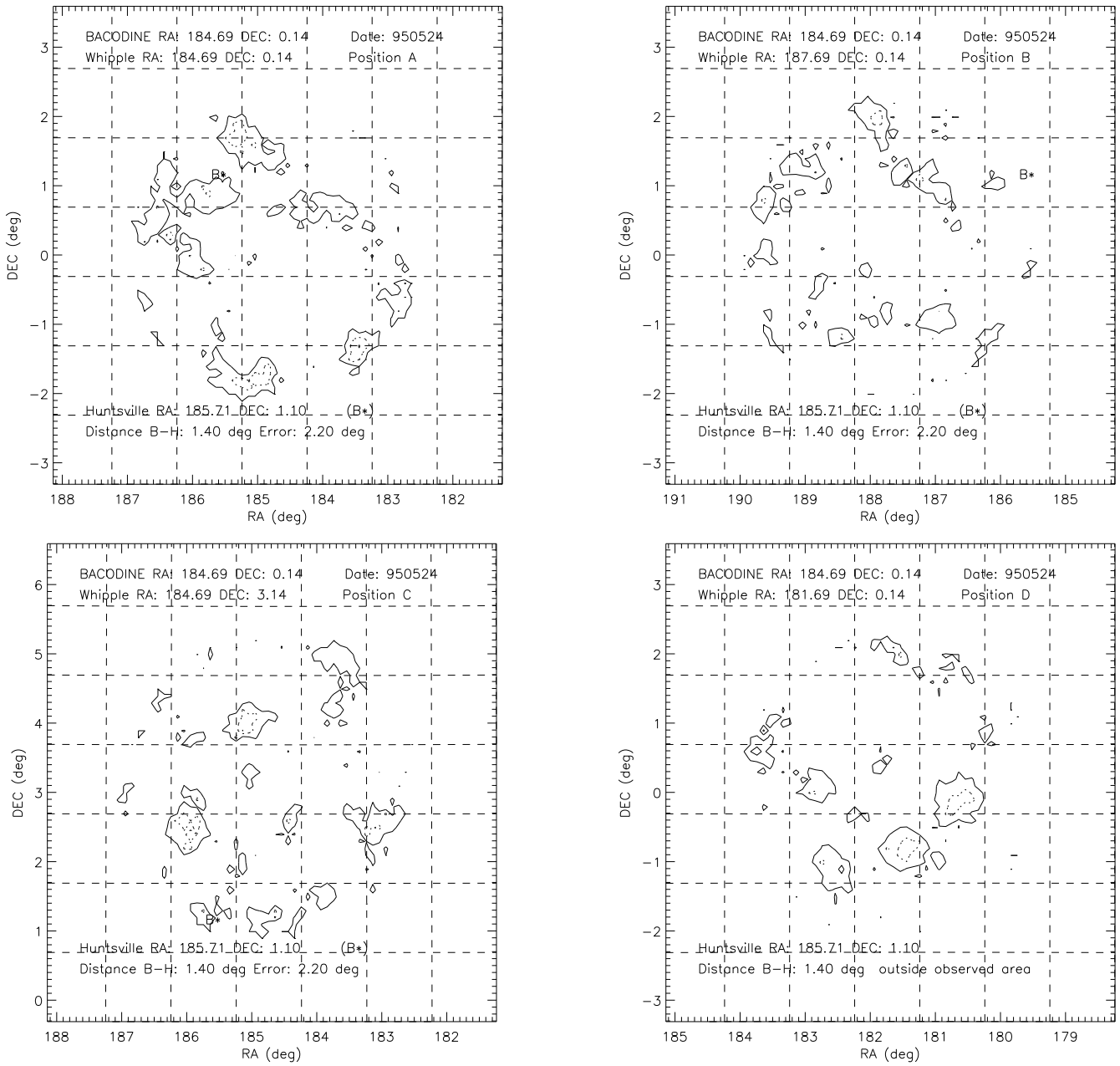

FIG. 3.—Bin excesses for the burst on 1995 May 24. The updated position of the burst is marked B* if it appears in the field of view.

each bin in the ON and OFF files, the excess in any bin, σ, can be defined as

$$\sigma(i, j) = \frac{N_{\mathrm{ON}(i,j)} - p \times N_{\mathrm{OFF}(i,j)}}{\sqrt{N_{\mathrm{ON}(i,j)} + p \times N_{\mathrm{OFF}(i,j)}}}, \quad (2)$$

where $N_{\mathrm{ON}(i,j)}$ and $N_{\mathrm{OFF}(i,j)}$ are the bin occupancies of grid position (i, j) in the data files taken on the night of the burst and the control night, respectively. A normalizing factor p, which is the ratio of shape-selected events in the ON to that in the OFF data, is applied to account for event rate variations due to differing sky conditions on the nights when the burst and control data were taken. While this will dilute the significance of any peak in the distribution for the night of the burst, it also reduces the chance of a spurious peak in the contour plot. The resulting contours on the grid represent the significances of the excess of photon-like events over 28 minutes on the night of the burst from each part of the camera.

Although the expected duration of the burst is not known, an excess of shape-selected events during a run or part of a run may merit further attention. The minute-by-minute rates of shape-selected events are calculated, and any excess over 3 σ over the mean for the data file is investigated.

3.4. *Sensitivity of Technique*

As a test of the sensitivity of the analysis technique, the method described above was applied to one Crab Nebula pair taken with the Crab offset 0°.4 from the center of the camera. The resulting grid is displayed in Figure 2, in which the contours represent values of $\sigma(i, j)$ from 1 to 5, with the

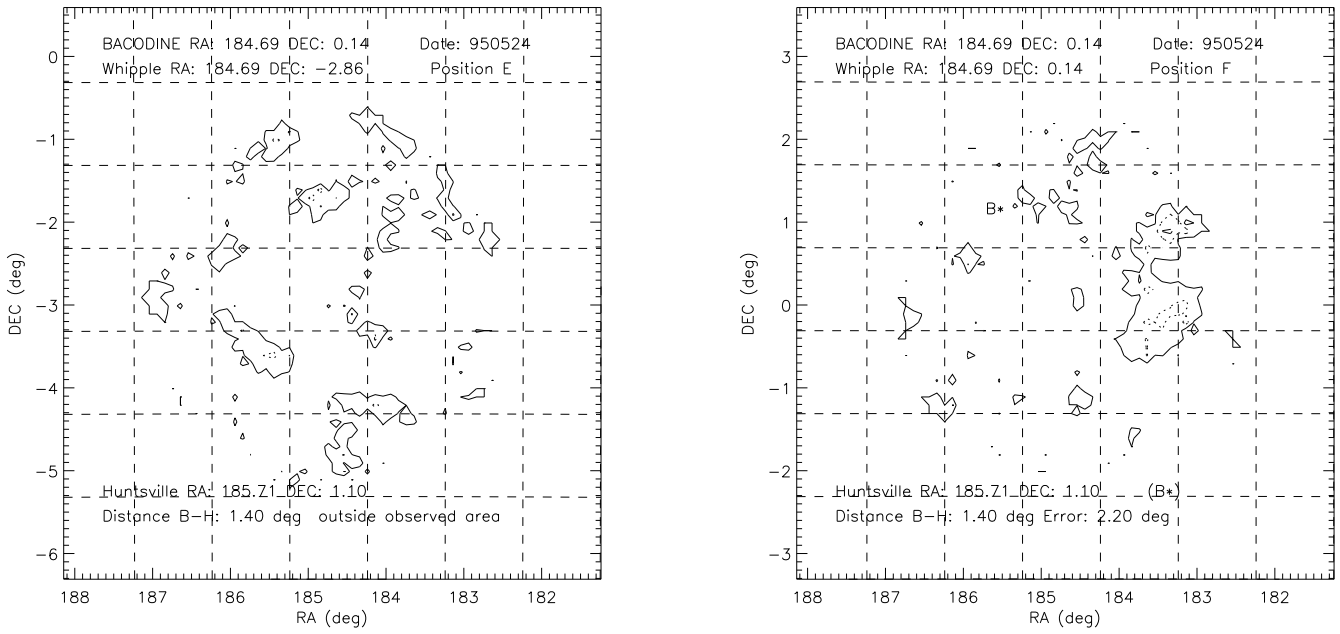

FIG. 3.—*Continued*

known position of the Crab Nebula consistent with the highest $\sigma(i, j)$ contours. Based on the number of bins ($\sim$1000), we expect to see, on average, one random 3 σ contour, so that the least significant excess detectable is therefore defined by a contour signaling a $\sigma(i, j) = 4$ contour. This corresponds numerically to less than the Crab Nebula flux over 28 minutes for a source at 0°.4 from the center of the field of view. If a $\sigma(i, j) = 4$ contour is seen farther away from the center of the camera where gamma-ray sensitivity is lower, then this flux limit is larger.

4. RESULTS

Figure 3 shows the contour plots for the ON/OFF pairs for the 1995 May 24 burst observed by the Whipple collaboration. The updated Huntsville burst position appears in four of the observed positions for these bursts and is marked by B*. The contours begin at 1 σ and increment in 1 σ steps.

Only the bins lying in a circle of radius 2° around the center of the field of view contain possible points of origin of events; calculations and significances are applied only to this region of each grid. The number of bins for each burst/control pair is therefore $\pi(2/0.1)^2 = 1257$.

If the spectrum for the burst recorded by BATSE, COMPTEL, and EGRET on 1994 February 17, in which GeV photons were recorded 1.5 hr after the end of the BATSE event, is extended to 0.3 TeV using the -2.5 spectrum given in Hurley et al. (1994a), then one obtains a fluence of 1.3×10^{-7} ergs cm^{-2} for emission at 0.3 TeV over a 28 minute period. Large uncertainties are associated with any EGRET burst spectra because of the small number of photons at the highest energies.

The collection area above 0.3 TeV of the 10 m telescope for a source in the center of the camera is $(5.4 \pm 0.9) \times 10^8$cm^2 (Connaughton et al. 1996). This is larger than the collection area given in, for example, Reynolds et al. (1993) because of the less restrictive orientation criteria applied to these non–source-centered observations. Given that there are no significant excesses in any of the bins in the ON data relative to the control data, one can calculate an upper limit to the flux from anywhere in the field of view for each of the scans on and around the burst position. Using the total number of shape-selected events in the ON and control files, the 99.9% maximum likelihood value for emission in position A of Figure 3 is $(1.6 \pm 0.3) \times 10^{-7}\gamma$ cm^{-2} or $(7.1 \pm 1.4) \times 10^{-8}$ ergs cm^{-2} over 28 minutes. This limit applies to extended or delayed emission above 0.3 TeV from a source in the center of the field of view. The limit for flux from any other observed point in the sky must be scaled over the field of view to account for the decreasing gamma-ray efficiencies away from the center of the camera. A lower flux upper limit is derived for bursters that might lie at the center of the camera than for those at the edge of the camera. A factor can be applied in accordance with the efficiencies defined in Connaughton et al. (1996) for off-center sensitivity. The upper limits to the delayed or extended emission above 0.3 TeV as a function of source offset for Position A of the 1995 May 24 burst are shown in Figure 4 (*solid line*). If, for

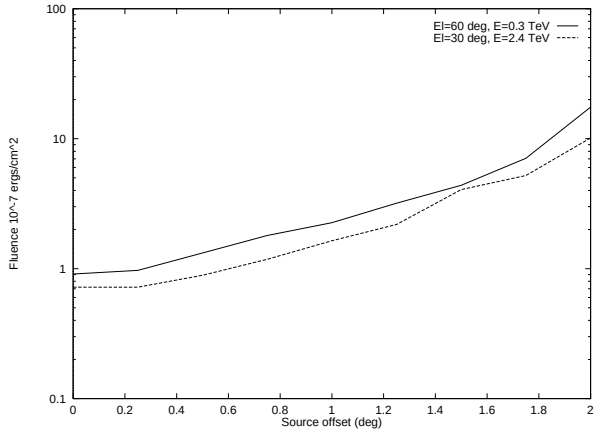

FIG. 4.—Upper limit to delayed or extended flux above 0.3 TeV for position A (*solid line*) and above 2.4 Tev for position F (*dashed line*) of the 1995 May 24 BATSE burst.

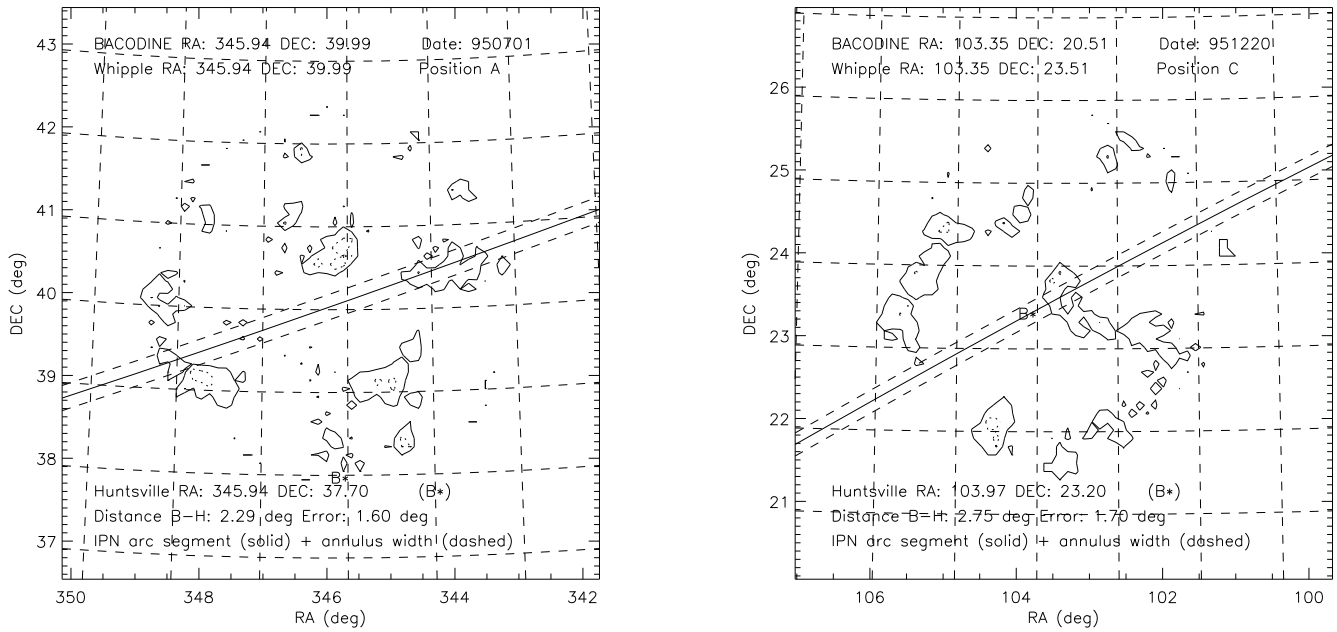

FIG. 5.—Bin excesses for position A of the 1995 July 1 and position C of the 1995 December 20 bursts. The updated position is marked B*, and the IPN arc derived from BATSE and *Ulysses* measurements is shown.

example, the burst of 1995 May 24 came from an observed location in position A in Figure 3, and if it emitted TeV gamma rays during the time between $T_{\rm BATSE}$ + 5 minutes and $T_{\rm BATSE}$ + 33 minutes, then the flux is lower than the above limit. Similar limits can be calculated from the data from the observations of positions B and C, which are also compatible with the error box of the updated BATSE position. The dashed line in Figure 4 applies to fluence limits for the final ON/OFF pair (position F), which was acquired at a telescope elevation of 30° and hence at a higher energy threshold (2–3 TeV) than the data taken above 50°.

The burst of 1995 July 1 has similar limits for TeV emission above 0.3 TeV within the statistical difference in event rates on 1995 May 24 and 1995 July 1 in the positions A, B, D, E, and F, which are compatible with the final Huntsville position. An additional 51 minutes must be added to the time during which each limit applies because of the longer delay in the Whipple response. Likewise, these limits can be derived for positions A, B, and C of the 1995 December 20 data. Both of these bursts had IPN arcs that intersected at least one of the positions observed by the Whipple collaboration, and Figure 5 shows two of the resulting contour plots.

An energy spectrum can be calculated for each burst in the BATSE energy range (~30–1800 keV) using Band's function (Band et al. 1993). This function yields a steeper spectrum above the peak power energy $E_{\rm peak}$ than below this energy, and the peak power and spectral indices can vary greatly between bursts. It is a huge extrapolation to extend the steep, power-law tail of the spectrum to TeV energies, but if this is done, then it can be seen that the Whipple upper limits for delayed or extended emission are of the order of that expected for prompt emission if the burst spectrum extends to TeV energies with no further breaks. These extrapolations are shown in Figure 6. Power-law indices of -2.48 ± 0.31, -2.38 ± 0.10, and -2.50 ± 0.25 are calculated from the BATSE data for the 1995 May 24, 1995 July 1, and 1995 December 20 bursts, respectively. In the case of the 1995 July 1 burst, the Whipple limit at 0.3 TeV is below the Band extrapolation, but it must be remembered that for this burst the Whipple observations began nearly 1 hr after the BATSE detection.

Although the updated locations from Huntsville fell more than 5° from the BACODINE coordinates in the bursts on 1995 April 5 and 1995 November 19, the BATSE error boxes were sufficiently large to incorporate the positions A, C, D, and F of 1995 November 19 and A and E of 1995 April 5. The fluence limits in Figure 4 apply to these positions (with corrections for the differences in event rates between the data sets), with low elevation limits applying to both positions observed on 950405. It was not possible to fit reliable spectra to these bursts from the BATSE data, as gaps in the telemetry prevented the construction of an adequate background model.

There was no evidence for any burstlike excess in any of the data taken on 1995 June 25, 1995 November 17, and 1995 November 24, but fluence limits are not relevant for the 1995 November 17 and 1995 November 24 observations, which missed the updated position of the burst by more than the BATSE error box. It is not currently possible to perform a complete analysis for the burst of 1995 June 25. Without control data, it is difficult to separate excesses from differences in sky brightness over the field of view. This problem is particularly difficult for the 1995 June 25 burst because of its location close to the Galactic center.

In the analysis described above, an excess of events from a particular area was sought over the duration of each observation run. An excess of gamma-ray shape-selected events over a subset of each 28 minute data file regardless of arrival direction was sought by examining minute-by-minute shape-selected event rates. Telescope elevation and sky brightness have a strong effect on event rates, but in spite of wide variations in shape-selected event rates between different observing runs, no statistically significant variations indicative of bursting activity can be seen within any run.

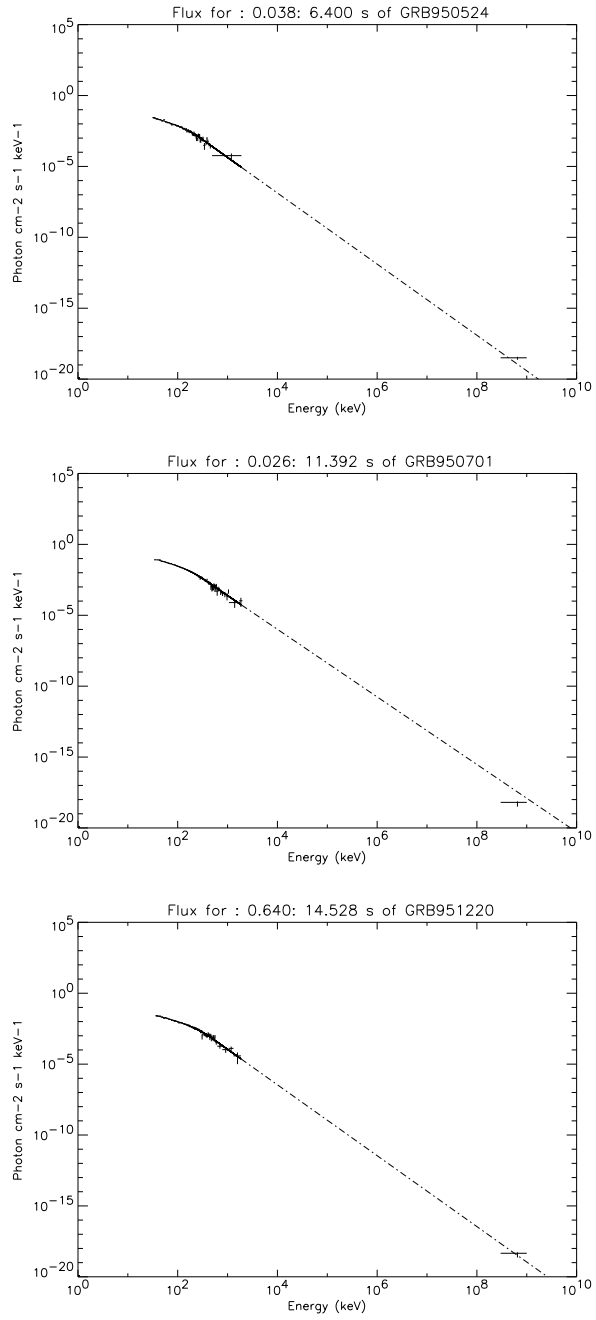

FIG. 6.—BATSE spectra for 1995 May 24, 1995 July 1, and 1995 December 20 bursts (Band model) extended to 1 TeV. The upper limit at 0.3 TeV is the Whipple result for a source at the center of the camera in position A of each set of observations. The dashed line is an extrapolation of the BATSE spectrum, which is calculated from photons of energy of approximately 30–1800 keV.

4.1. *Future Prospects*

The overlap between Whipple collaboration observations and BATSE burst positions in space and almost in time made possible by the distribution of burst coordinates through BACODINE has provided upper limits to the delayed fluence above TeV from nearby GRB that are more restrictive than suggested by EGRET observations at 18 GeV. If the burst positions observed by the Whipple collaboration contain galactic or near-cosmological burst sources emitting at times between 5 minutes and 3 hr after the BATSE trigger, and the spectra are similar to the EGRET-detected burst on 1994 February 17, then the emission spectra above GeV energies must be at least as steep as at BATSE energies and the fluence lower than that obtained by extrapolating the EGRET fluence for the 1994 February 17 event to 0.3 TeV with the -2.5 slope inferred from that event.

While the duty cycle of the visible Cherenkov technique is limited by weather and moon cycles, the slew time is currently 5 times faster than in 1994 May, with the addition last year of the fast slew capability to the azimuth motor. Sky coverage should be enhanced by the operation of a second reflector, 11 m in diameter, located 120 m away from the 10-m reflector. This could double sky coverage during BACODINE responses if both reflectors were deployed to cover different parts of the 9° diameter area currently observed over the 3 hr response cycle. Alternatively, the deployment of the 11 m reflector in coincidence with the 10 m would improve the sensitivity of the technique by providing a unique point of origin for about 40% of showers.

A project is being undertaken that will expand the focus box of the 10 m reflector with two outer rings of large phototubes. A field of view of 6°.5 will greatly increase the chance that the final burst position was probed during the first 28 minute BACODINE observation. It will also provide more efficient non–source-centered analysis techniques.

We acknowledge the technical assistance of Teresa Lappin and Kevin Harris. We thank the referee, Kevin Hurley, for helpful suggestions and Michael Briggs, Bob Mallozzi, and Rob Preece for assistance with WINGSPAN spectral fitting software. This research is supported by grants from the US Department of Energy and by NASA, PPARC in the UK, and Forbairt in Ireland.

REFERENCES

Akerlof, C., et al. 1991, ApJ, 377, L97
———. 1994, AIP Conf. Proc. 307, Gamma-Ray Bursts, ed. G. J. Fishman, J. J. Brainerd, & K. Hurley (New York: AIP), 633
———. 1995, Ap&SS, 231, 255
Band, D., et al. 1993, ApJ, 413, 281
Barthelmy, S., et al. 1994, AIP Conf. Proc. 307, Gamma-Ray Bursts, ed. G. J. Fishman, J. J. Brainerd, & K. Hurley (New York: AIP), 643
Cawley, M. F., & Weekes, T. C. 1995, Exp. Astron., 6, 7
Chantell, M., et al. 1995, Proc. 24th Int. Cosmic-Ray Conf. (Rome), 2, 544
Cohen, E., & Piran, T. 1995, ApJ, 444, L25
Connaughton, V., et al. 1994, AIP Conf. Proc. 307, Gamma-Ray Bursts, ed. G. J. Fishman, J. J. Brainerd, & K. Hurley (New York: AIP), 470
Connaughton, V., et al. 1996, Astropart. Phys., submitted
Dingus, B. L., et al. 1994, AIP Conf. Proc. 307, Gamma-Ray Bursts, ed. G. J. Fishman, J. J. Brainerd, & K. Hurley (New York: AIP), 22
Edwards, P. G., et al. 1995, Proc. 24th Int. Cosmic-Ray Conf. (Rome), 2, 120
Fenimore, E. E., & Bloom, J. S. 1995, ApJ, 453, 25
Horack, J. M., Emslie, A. G., & Hartmann, D. H. 1995, ApJ, 447, 474
Hurley, K. 1996, Space Sci. Rev., 75, 43
Hurley, K., et al. 1994a, Nature, 372, 652
———. 1994b, AIP Conf. Proc. 307, Gamma-Ray Bursts, ed. G. J. Fishman, J. J. Brainerd, & K. Hurley (New York: AIP), 27
Kifune, T., et al. 1993, Proc. 23d Int. Cosmic-Ray Conf. (Calgary), 1, 444
Krennrich, F. K., et al. 1997, ApJ, in press

Lessard, R. L., et al. 1996, in preparation
Mannheim, K., Hartmann, D., & Funk, B. 1996, ApJ, 467, 532
Norris, J. P., et al. 1994, ApJ, 424, 540
———. 1995, ApJ, 439, 542
Plunkett, S. P., et al. 1995, Ap&SS, 231, 271
Reynolds, P. T., et al. 1993, ApJ, 404, 206
Schaefer, B. E. 1994, AIP Conf. Proc. 307, Gamma-Ray Bursts, ed. G. J. Fishman, J. J. Brainerd, & K. Hurley (New York: AIP), 382
Stecker, F. W., et al. 1992, ApJ, 390, L49